Two bHLH Transcription Factors, bHLH34 and bHLH104, Regulate Iron Homeostasis in *Arabidopsis thaliana*[1]

Xiaoli Li, Huimin Zhang, Qin Ai, Gang Liang*, and Diqiu Yu*

School of Life Sciences, University of Science and Technology of China, Hefei, Anhui 230027, China (X.L., H.Z.); Key Laboratory of Tropical Plant Resources and Sustainable Use, Xishuangbanna Tropical Botanical Garden, Kunming, Yunnan 650223, China (X.L., H.Z., Q.A., G.L., D.Y.); and University of the Chinese Academy of Sciences, Beijing 100049, China (Q.A.)

ORCID ID: 0000-0002-0622-4043 (G.L.).

The regulation of iron (Fe) homeostasis is critical for plant survival. Although the systems responsible for the reduction, uptake, and translocation of Fe have been described, the molecular mechanism by which plants sense Fe status and coordinate the expression of Fe deficiency-responsive genes is largely unknown. Here, we report that two basic helix-loop-helix-type transcription factors, bHLH34 and bHLH104, positively regulate Fe homeostasis in Arabidopsis (*Arabidopsis thaliana*). Loss of function of bHLH34 and bHLH104 causes disruption of the Fe deficiency response and the reduction of Fe content, whereas overexpression plants constitutively promote the expression of Fe deficiency-responsive genes and Fe accumulation. Further analysis indicates that bHLH34 and bHLH104 directly activate the transcription of the Ib subgroup *bHLH* genes, *bHLH38/39/100/101*. Moreover, overexpression of *bHLH101* partially rescues the Fe deficiency phenotypes of *bhlh34bhlh104* double mutants. Further investigation suggests that bHLH34, bHLH104, and bHLH105 (IAA-LEUCINE RESISTANT3) function as homodimers or heterodimers to nonredundantly regulate Fe homeostasis. This work reveals that plants have evolved complex molecular mechanisms to regulate Fe deficiency response genes to adapt to Fe deficiency conditions.

Iron (Fe) is of particular importance as a cofactor for a wide variety of proteins in living organisms. In humans, Fe deficiency is one of the major reasons for anemia. A plant diet is a major resource for humans; thus, it is important to clarify the mechanisms of Fe homeostasis in plants. Fe is an indispensable micronutrient for plant growth and development and is involved in many cellular functions, including chlorophyll biosynthesis, photosynthesis, and respiration (Hänsch and Mendel, 2009). Therefore, a decrease in Fe uptake directly affects crop yield and crop quality. Plants take up Fe from the soil, but Fe availability is limited, as its major form is as insoluble ferric hydroxides, especially in calcareous soils, which make up one-third of the world's cultivated areas.

To cope with low-Fe environments, higher plants have evolved two major strategies for Fe acquisition. Nongraminaceous plants employ a reduction strategy (strategy I) that involves three stages in low-Fe conditions. The acidification of soil by protons extruded by H^+-ATPases and phenolic compounds makes Fe(III) more soluble (Santi and Schmidt, 2009; Kobayashi and Nishizawa, 2012). The ferric chelate reductase activity of FERRIC REDUCTION OXIDASE2 (FRO2) is induced by low Fe; this enzyme reduces Fe(III) to Fe(II) (Robinson et al., 1999). The Fe(II) is then transported into roots by the major Fe transporter of plant roots, IRON-REGULATED TRANSPORTER1 (IRT1; Eide et al., 1996; Henriques et al., 2002; Varotto et al., 2002; Vert et al., 2002). In contrast, graminaceous plants use a chelation-based strategy (strategy II; Walker and Connolly, 2008; Morrissey and Guerinot, 2009). These plants release mugineic acid family phytosiderophores, which have high affinity for Fe(III) and efficiently bind Fe(III) in the rhizosphere. The resulting chelate complexes are then transported into plant roots via a specific transport system (Mori, 1999).

The transcriptional regulation of genes involved in Fe uptake under Fe-deficient conditions is intensively controlled by plants. In the past decade, several basic helix-loop-helix (bHLH) proteins have been identified as regulators of the Fe deficiency response. The bHLH protein in tomato (*Solanum lycopersicum*), FER, was the first characterized to control Fe deficiency responses, and its mutant failed to activate Fe acquisition strategy I (Ling et al., 2002). FE-DEFICIENCY INDUCED TRANSCRIPTION FACTOR (FIT), a homolog of FER in Arabidopsis (*Arabidopsis*

[1] This work was supported by the Youth Innovation Promotion Association of the Chinese Academy of Sciences, the Candidates of the Young and Middle Aged Academic Leaders of Yunnan Province (grant no. 2015HB095), and the Program for the Innovative Research Team of Yunnan Province (grant no. 2014HC017).

* Address correspondence to lianggang@xtbg.ac.cn and ydq@xtbg.ac.cn.

The author responsible for distribution of materials integral to the findings presented in this article in accordance with the policy described in the Instructions for Authors (www.plantphysiol.org) is: Gang Liang (lianggang@xtbg.ac.cn).

X.L., G.L., and D.Y. designed the study; X.L., H.Z., Q.A., and G.L. performed research; X.L., H.Z., G.L., and D.Y. analyzed data; G.L. wrote the article; X.L., G.L., H.Z., Q.A., and D.Y. revised the article; all authors read and approved the final article.

www.plantphysiol.org/cgi/doi/10.1104/pp.15.01827

thaliana), is required for the proper regulation of ferric chelate reductase activity and Fe transport into the plant root, and its mutation was lethal when plants were grown in normal soils (Colangelo and Guerinot, 2004; Jakoby et al., 2004; Yuan et al., 2005). However, overexpression of *FIT* is not sufficient to constitutively induce the expression of its target genes, such as *IRT1* and *FRO2*, in normal growth conditions. In fact, FIT is dually regulated by Fe starvation. At the transcriptional level, FIT is induced by Fe deficiency (Colangelo and Guerinot, 2004; Jakoby et al., 2004; Yuan et al., 2005). At the posttranscriptional level, FIT is actively destabilized and degraded by the 26S proteasome during Fe limitation (Meiser et al., 2011; Sivitz et al., 2011). In addition, FIT can form a heterodimer with members of the Ib subgroup of bHLH proteins (bHLH38/39/100/101) to constitutively activate the transcription of *IRT1* and *FRO2* (Yuan et al., 2008; Wang et al., 2013). Both FIT and bHLH38/39/100/101 function as positive regulators. In contrast, POPEYE (PYE) was identified as playing a negative role in the Fe deficiency response in Arabidopsis (Long et al., 2010). *PYE* transcript levels were elevated when plants were subjected to low-Fe conditions. Chip-on-chip experiments revealed that PYE directly targets several genes involved in metal homeostasis, such as *NICOTIANAMINE SYNTHASE4* (*NAS4*), *FRO3*, and *ZINC-INDUCED FACILITATOR1* (*ZIF1*). In a *pye1* mutant, the expression of these target genes is significantly up-regulated in Fe-deficient conditions, suggesting that PYE functions as a negative regulator.

It is unclear how plants perceive Fe status and transmit signals to downstream pathways. In mammals, FBXL5 functions as an Fe sensor and contains a hemerythrin domain (HHE) for Fe binding and an F-box domain for the ubiquitination and degradation of IRP2. The latter governs cellular Fe homeostasis by regulation of the translation and stability of mRNAs involved in Fe homeostasis (Salahudeen et al., 2009; Vashisht et al., 2009). Interestingly, two different groups (Kobayashi et al., 2013; Selote et al., 2015) confirmed that Arabidopsis BRUTUS (BTS) and its rice (*Oryza sativa*) orthologs, HAEMERYTHRIN MOTIF-CONTAINING REALLY INTERESTING NEW GENE (RING) AND ZINC-FINGER PROTEIN1 (HRZ1) and HRZ2, possess HHE domains for binding Fe. Although they lack an F-box domain similar to that in FBXL5, BTS and HRZ1/2 have RING domains that can mediate the ubiquitination reaction. Functional analysis revealed that BTS and HRZ1/2 negatively regulate the Fe deficiency response in plants. Given that BTS and HRZ1/2 are structurally and functionally similar to FBXL5, they are thought to be potential Fe sensors in plants. Although no substrates for HRZ1/2 have been found, it is established that BTS interacts with three PYE-like proteins (bHLH104, bHLH105/ILR3, and bHLH115) and facilitates the 26S proteasome-mediated degradation of bHLH105/IAA-LEUCINE RESISTANT3 (ILR3) and bHLH115 in the absence of Fe in vitro (Selote et al., 2015). Recently, Zhang et al. (2015) revealed that bHLH104 and bHLH105 positively regulate Fe homeostasis by directly activating the transcription of *bHLH38/39/100/101* and *PYE*. Further investigation is required to explore the functions of the other PYE-like proteins.

Here, through screening regulators upstream of *bHLH101*, we identified the bHLH transcription factor bHLH34, a homolog of bHLH104 in Arabidopsis. Mutational analysis suggests that bHLH34 and bHLH104 positively regulate the Fe deficiency response. Further analysis reveals that both bHLH34 and bHLH104 directly activate the transcription of *bHLH38/39/100/101*. In agreement with this, constitutive expression of *bHLH101* partially complements the Fe deficiency symptoms of *bhlh34bhlh104* double mutants. Protein interaction assays indicate that both heterodimers and homodimers occur between bHLH34, bHLH104, and bHLH105. These data reveal that bHLH34 and bHLH104 play major roles in regulating Fe homeostasis by activating the transcription of bHLH38/39/100/101 under Fe deficiency conditions.

RESULTS

Identification of *bHLH34*

bHLH38/39/100/101 have been characterized as key transcription factors regulating the Fe-deficient response in Arabidopsis, and their transcript levels are also up-regulated by Fe deficiency. To identify transcription factors functioning upstream of *bHLH38/39/100/101*, yeast one-hybrid screening was performed using the promoter of *bHLH101* as bait. From the screening, we obtained nine positive colonies, three of which encoded a bHLH protein, bHLH34. As a close homolog of bHLH34 (Supplemental Fig. S1), bHLH104 has been characterized to bind the promoter of *bHLH101* (Zhang et al., 2015). Further experiments confirmed that both bHLH34 and bHLH104, but not the other candidates, can activate the promoter of *bHLH101* (Fig. 1), which suggests that both bHLH34 and bHLH104 regulate the *bHLH101* gene. Given that other Fe homeostasis-associated transcription factors, such as *bHLH38/39/100/101*, *FIT*, *PYE*, and *MYB10/72*, are induced by Fe deficiency, we wanted to know whether *bHLH34* and

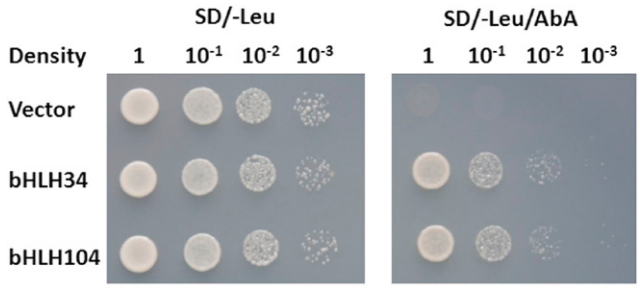

Figure 1. Identification of *bHLH34* and *bHLH104* by yeast one-hybrid assay. The promoter of *bHLH101* was used as bait and bHLH34/104 as prey. The representative growth status of yeast cells is shown on synthetic dextrose medium agar plates without Leu (SD/-Leu) with or without aureobasidin A (AbA) from triplicate independent trails.

bHLH104 are also responsive to Fe deficiency. Transcript abundance analysis indicated that neither *bHLH34* nor *bHLH104* is affected by Fe deficiency (Supplemental Fig. S2).

bhlh34, *bhlh104*, and *bhlh34bhlh104* Mutant Plants Display Fe Deficiency Symptoms

To investigate the functions of *bHLH34* and *bHLH104*, two transfer DNA (T-DNA) insertion alleles for the *bHLH34* and *bHLH104* genes were obtained from The Arabidopsis Information Resource (TAIR). *bhlh34* contains a T-DNA insertion in the second exon and *bhlh104* has a T-DNA insertion in the third intron (Fig. 2A). The homozygous lines of *bhlh34* and *bhlh104* were isolated by PCR, and the positions of the insertions were confirmed. The loss of full-length transcripts in the T-DNA lines were determined by reverse transcription-PCR (Fig. 2B), indicating that both T-DNA lines are knockout mutants. Considering their putative functional redundancy, we constructed *bhlh34bhlh104* double mutants by crossing two single knockout mutants. When grown on Fe-sufficient medium, neither single mutants nor double mutants showed any obvious phenotypic differences compared with wild-type plants (Supplemental Fig. S3). However, when they were grown on Fe-free medium, all mutants displayed Fe-deficient symptoms, and the double mutants had the most severe phenotypes (Fig. 2C).

To further confirm the functions of bHLH34 and bHLH104, we designed an artificial microRNA, *amiR-bhlh34/104*, which is predicted to target both *bHLH34* and *bHLH104* (Supplemental Fig. S4A), and generated *amiR-bhlh34/104* transgenic plants. Quantitative reverse transcription-PCR analysis demonstrated that both *bHLH34* and *bHLH104* were significantly downregulated in *amiR-bhlh34/104* plants (Supplemental Fig. S4B). As expected, the *amiR-bhlh34/104* transgenic plants grown in soils showed interveinal chlorosis in leaves, which is very similar to that of *bhlh34bhlh104* double mutants (Fig. 2D). Further phenotype evaluation revealed that the root growth of *amiR-bhlh34/104* seedlings was strongly inhibited on Fe-deficient medium, whereas no visible difference was observed between *amiR-bhlh34/104* and wild-type plants on normal medium (Supplemental Fig. S4, C and D). These results demonstrate that the *amiR-bhlh34/104* plants phenocopy the *bhlh34bhlh104* mutants.

Impaired Fe Deficiency Response by Loss of Function of bHLH34 and bHLH104

We further determined the Fe-associated phenotypes of plants grown in soils containing various concentrations of calcium oxide (Fig. 3A), which was used to produce alkaline soil in which the Fe availability was limited because of decreased Fe solubility. In normal soil, no visible phenotypic difference was observed between the *bhlh34*, *bhlh104*, and wild-type plants, whereas the *bhlh34bhlh104* double mutants had small

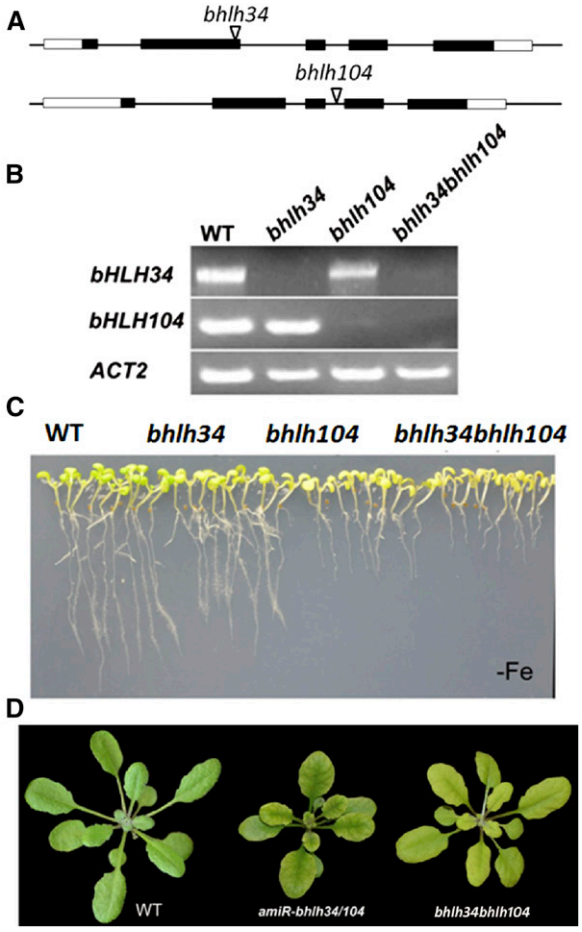

Figure 2. Characterization of various mutant plants. A, T-DNA insertion position in the corresponding gene. Black boxes indicate the coding sequence. White boxes indicate untranslated regions. Triangles indicate the position of T-DNA. B, The corresponding full-length complementary DNAs (cDNAs) were amplified by reverse transcription-PCR to confirm the mutants. C, Ten-day-old seedlings germinated directly on Fe-deficient (–Fe) medium. D, Phenotypes of *amiR-bhlh34/104* and *bhlh34bhlh104* plants in soils. Four-week-old plants grown in normal soil are shown. WT, Wild type.

stature and chlorotic leaves. In soil supplemented with 1‰ (w/w) calcium oxide, the *bhlh104* mutants showed slight chlorosis. In contrast, 5‰ (w/w) calcium oxide caused leaf chlorosis in all three types of mutants and seedling lethality of the *bhlh34bhlh104* double mutants. These data suggest that the loss of function of bHLH34 and bHLH104 inhibits the Fe deficiency response of the *bhlh34bhlh104* plants.

Fe is indispensable for the synthesis of chlorophyll, and Fe deficiency often causes leaf chlorosis with decreased levels of chlorophyll in plants (Terry, 1980). The significant chlorosis of the *bhlh34bhlh104* double mutant plants implied a decline in chlorophyll content. We measured chlorophyll levels in plants grown on Fe-sufficient and Fe-deficient media. There were no significant differences under Fe-sufficient conditions. However, under Fe-deficient conditions, the mutants

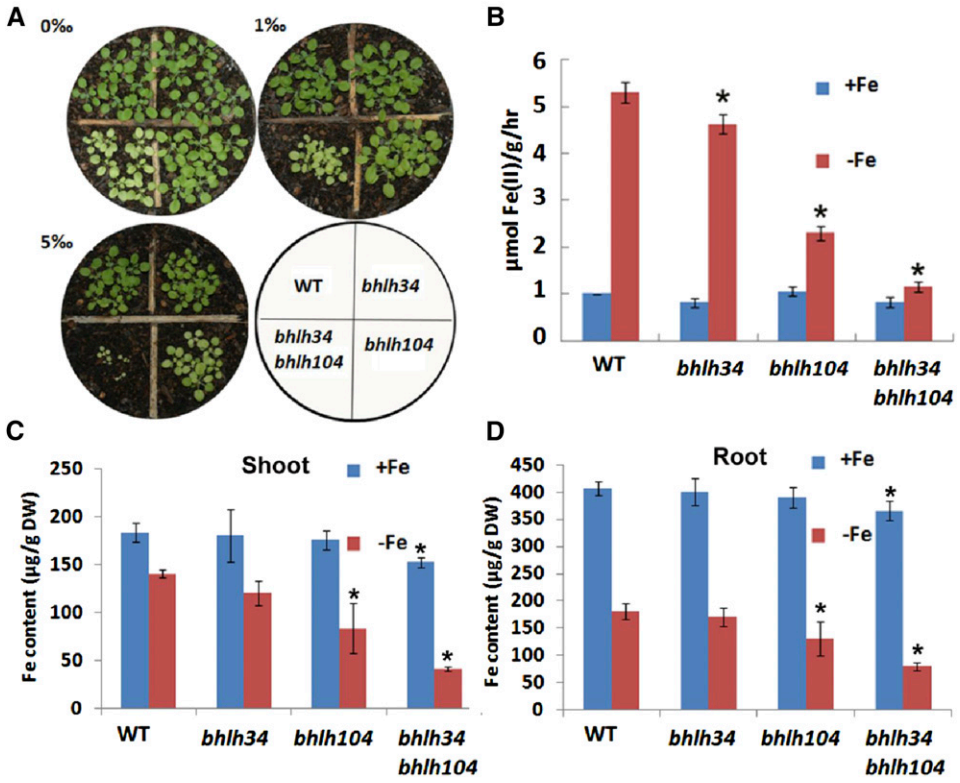

Figure 3. Fe deficiency response of various mutants. A, Three-week-old plants germinated in soil with various concentrations of calcium oxide. B, Iron reductase activity of plants germinated and grown on Fe-sufficient (+Fe) medium for 10 d and then shifted to Fe-deficient (–Fe) medium for 3 d. The ferrozine assay was performed, in triplicate, on 10 pooled plant roots. Significant differences from the wild type (WT) are indicated by asterisks ($P < 0.05$). C and D, Fe content of shoots and roots. Seedlings were germinated and grown on +Fe medium for 11 d and then shifted to +Fe or –Fe medium for 3 d. Significant differences from the wild type are indicated by asterisks ($P < 0.05$). DW, Dry weight.

showed significantly reduced chlorophyll levels, and the *bhlh34bhlh104* double mutants had the lowest chlorophyll levels (Supplemental Fig. S5).

Fe reductase activity is a typical indicator of Fe deficiency. We analyzed Fe reductase activity using the ferrozine assay (Yi and Guerinot, 1996). In Fe-sufficient conditions, no significant difference in Fe reductase activity was observed between wild-type and mutant plants. In response to Fe deficiency, both wild-type and mutant plants increased their Fe reductase activity. However, the Fe reductase activity of the mutant plants was significantly lower than that of wild-type plants, and the *bhlh34bhlh104* double mutants had the lowest Fe reductase activity (Fig. 3B).

To determine whether the loss of function of *bHLH34* and *bHLH104* causes altered Fe accumulation, the Fe content of wild-type and mutant 2-week-old seedlings was measured. Eleven-day-old seedlings grown under Fe-sufficient conditions were transferred to Fe-sufficient or Fe-deficient medium for another 3 d. Roots and shoots were harvested separately and used for Fe content analysis. The shoots of *bhlh34bhlh104* plants had 17% less Fe than the shoots of wild-type plants under Fe-sufficient conditions and 71% less Fe under Fe-deficient conditions (Fig. 3C). Similar results also were observed in roots. The roots of *bhlh34bhlh104* plants contained 10% less Fe than the roots of wild-type plants under Fe-sufficient conditions and 56% less Fe under Fe-deficient conditions (Fig. 3D). These data suggest that *bHLH34* and *bHLH104* are required to maintain Fe homeostasis in both Fe-sufficient and Fe-deficient conditions.

Fe Deficiency-Responsive Genes Are Down-Regulated in the *bhlh34*, *bhlh104*, and *bhlh34bhlh104* Mutants

To adapt to Fe-deficient conditions, plants often elevate the expression of Fe uptake-associated genes. Fe deficiency-induced genes *FRO2* and *IRT1* encode two key root membrane proteins for Fe homeostasis; the former converts Fe(III) to Fe(II), and the latter transports ferrous Fe from soil to root (Robinson et al., 1999; Vert et al., 2002). Given the low Fe levels in the *bhlh34bhlh104* mutants, we wanted to know whether the expression of these two Fe uptake-associated genes is altered in the mutants. In response to Fe deficiency, both genes were induced in the roots of wild-type and mutant plants. However, their expression levels were low in the mutants compared with the wild type under both Fe-sufficient and Fe-deficient conditions (Fig. 4). Moreover, their expression levels in *bhlh34bhlh104* under Fe-deficient conditions were close to that in the wild type in Fe-sufficient conditions. These alterations suggest that there is decreased Fe uptake in the mutant plants, which is in agreement with the reduction in both Fe reductase activity and Fe accumulation. These data also demonstrate that bHLH34 and bHLH104 directly or indirectly activate the expression of *FRO2* and *IRT1*.

Two MYB transcription factors, *MYB10* and *MYB72*, were identified as Fe deficiency-responsive genes, which are responsible for the activation of expression of the *NAS4* gene in Fe-deficient conditions in Arabidopsis (Palmer et al., 2013). Considering the fact that the *bhlh34bhlh104* mutants display interveinal chlorosis

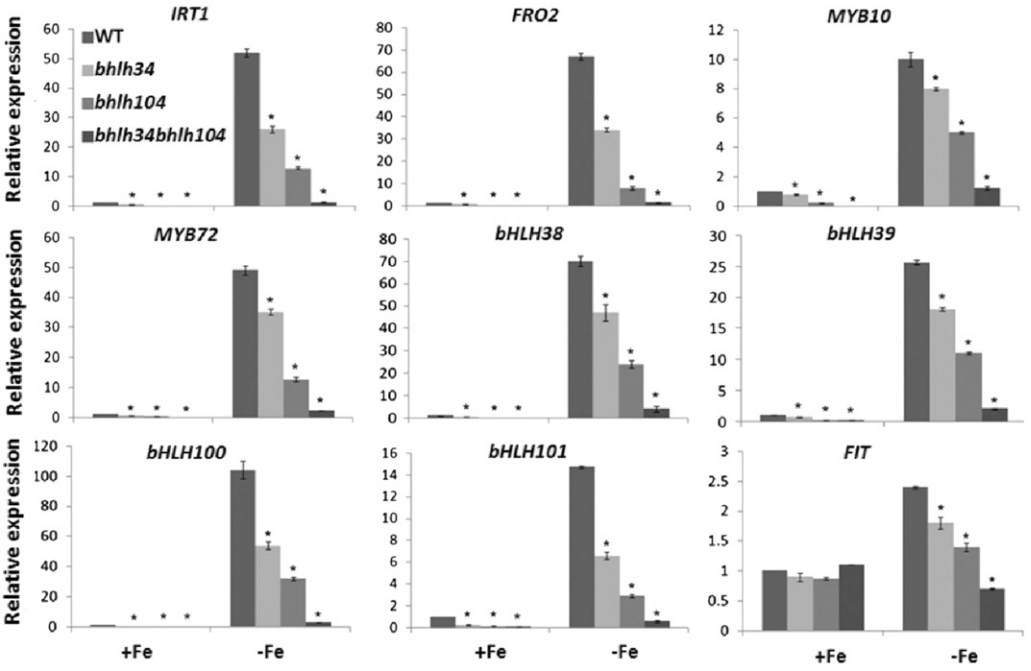

Figure 4. Expression of Fe deficiency-responsive genes in various mutants. Wild-type (WT) and mutant plants were grown on Fe-sufficient (+Fe) medium for 10 d and then transferred to +Fe or Fe-deficient (–Fe) medium for 3 d. RNA was prepared from root tissues. The data represent means ± SD of three technical repeats from one representative experiment. Significant differences from the corresponding wild type are indicated by asterisks ($P < 0.05$). DW, Dry weight.

similar to *nas4x-1* mutants (Klatte et al., 2009), we asked whether these two *MYB* genes are affected in the *bhlh34bhlh104* mutants. As expected, compared with the wild type, the mutants show considerably down-regulated transcript abundance of *MYB10* and *MYB72* regardless of whether Fe is deficient or not (Fig. 4), suggesting that bHLH34 and bHLH104 positively regulate the transcription of *MYB10* and *MYB72*.

The well-known transcription factors for Fe homeostasis in Arabidopsis are four Ib subgroup bHLH transcription factors (*bHLH38/39/100/101*) and another bHLH transcription factor, *FIT*, all of which are induced by Fe deficiency (Colangelo and Guerinot, 2004; Wang et al., 2007). Each of bHLH38/39/100/101 can interact with FIT to regulate the expression of Fe uptake-associated genes (Yuan et al., 2008; Wang et al., 2013). To determine the position of bHLH34 and bHLH104 in Fe signaling pathways, it is necessary to investigate their regulatory relationship with these bHLH transcription factors. Gene expression analysis revealed that *bHLH38/39/100/101* were strongly down-regulated in the *bhlh34bhlh104* mutants under both Fe-sufficient and Fe-deficient conditions, whereas *FIT* was moderately decreased (Fig. 4). These data imply that bHLH34 and bHLH104 act upstream of *bHLH38/39/100/101* and *FIT*.

In addition, we also determined the expression of genes that are involved in Fe distribution in plants, finding that *NAS2*, *NAS4*, *ZIF1*, *FRD3*, *OPT3*, and *PYE* were down-regulated in the *bhlh34bhlh104* mutants in response to Fe deficiency (Supplemental Fig. S6). Taken together, our data suggest that bHLH34 and bHLH104 positively regulate the Fe deficiency response.

Overexpression of *bHLH34* and *bHLH104* Activates the Fe Deficiency Response

Considering the inhibited Fe deficiency response caused by the loss of function of *bHLH34* and *bHLH104*, we asked whether elevated expression of *bHLH34* and *bHLH104* would enhance the Fe deficiency response. First, we performed complementation assays. Pro_{bHLH34}:*Myc-bHLH34* and $Pro_{bHLH104}$:*Myc-bHLH104* constructs were introduced into the *bhlh34* and *bhlh104* mutants, respectively. When grown on Fe deficiency medium, both Pro_{bHLH34}:*Myc-bHLH34/bhlh34* and $Pro_{bHLH104}$:*Myc-bHLH104/bhlh104* plants were comparable with wild-type plants (Supplemental Fig. S7), suggesting that both mutants were rescued. Next, we constructed transgenic plants expressing Pro_{35S}:*Myc-bHLH34* and Pro_{35S}:*Myc-bHLH104*. When grown in normal soils, about 10% of Pro_{35S}:*Myc-bHLH34* and 33% of Pro_{35S}:*Myc-bHLH104* T0 transgenic plants displayed visible phenotypes (small rosettes and leaf necrosis; Fig. 5A), and no visible phenotype was observed for the other transgenic plants. We further assessed the root phenotypes of T1 plants when grown on Fe deficiency medium, finding that the progeny of T0 plants with visible phenotypes produced short roots whereas the root length of the other progeny was similar to that of wild-type plants (Fig. 5B). In contrast, no

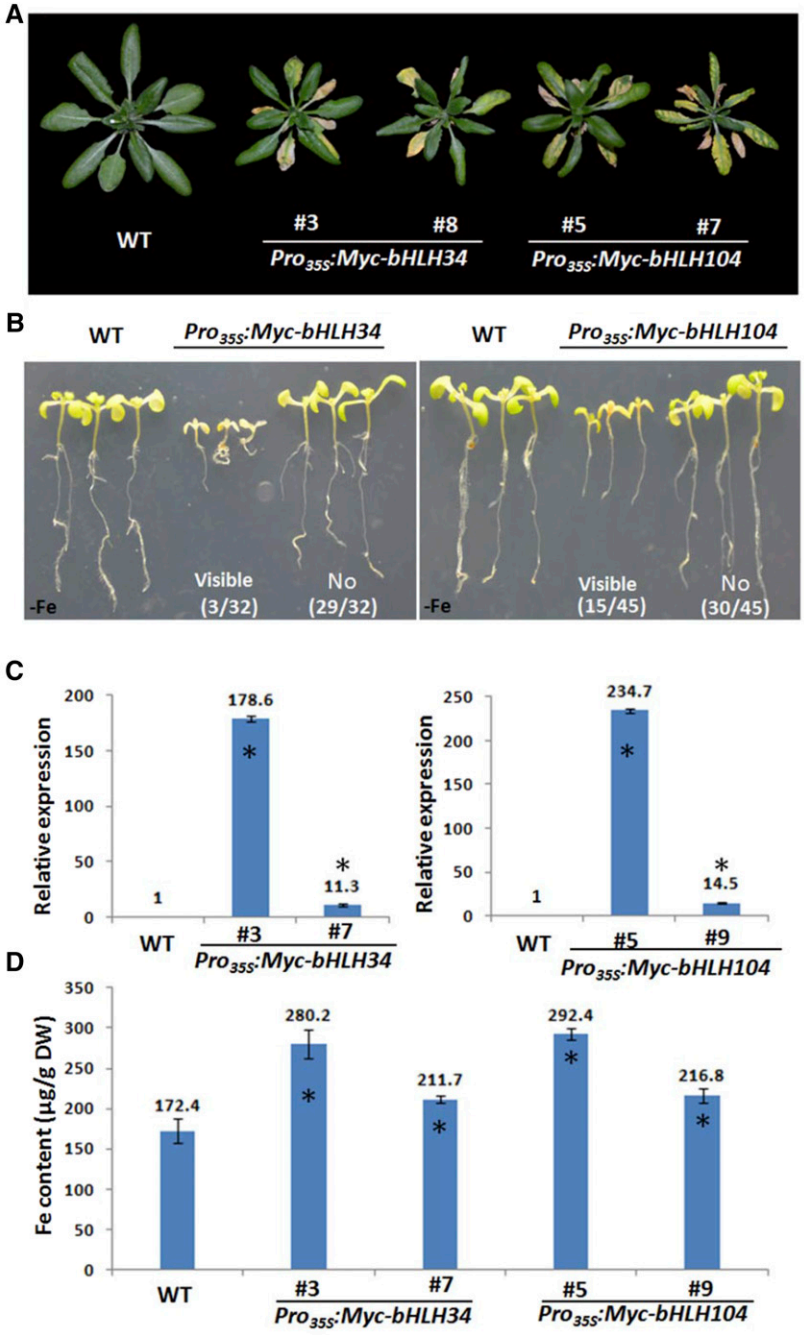

Figure 5. Phenotypes of *bHLH34* and *bHLH104* overexpression plants. A, Four-week-old plants grown in normal soil. B, Ten-day-old seedlings grown on Fe-deficient (–Fe) medium. Numbers indicate the frequency of transgenic plants with the corresponding phenotypes. C, Relative transcript levels of *bHLH34* (left) and *bHLH104* (right) in overexpression plants. Significant differences from the wild type (WT) are indicated by asterisks ($P < 0.05$). D, Fe content of leaves in 4-week-old plants grown in normal soil. Significant differences from the wild type are indicated by asterisks ($P < 0.05$). DW, Dry weight.

visible phenotypes were observed between wild-type and transgenic plants when grown on Fe-sufficient medium for 10 d (Supplemental Fig. S8A). The determination of transgene abundance revealed that the transgenic plants with visible phenotypes have significantly higher transgene levels than those without visible phenotypes (Fig. 5C; Supplemental Fig. S8B), suggesting that the visible phenotypes are closely associated with the transgene levels. For further investigation, *Pro$_{35S}$:Myc-bHLH34#3* and *Pro$_{35S}$:Myc-bHLH104#5* were chosen as representatives of plants with visible phenotypes and *Pro$_{35S}$:Myc-bHLH34#7* and *Pro$_{35S}$:Myc-bHLH104#9* as representatives of plants without visible phenotypes.

Given that the *bhlh34bhlh104* mutants contain less Fe than the wild type, we asked whether overexpression transgenic plants accumulate more Fe than wild-type plants. The leaves of 4-week-old plants grown in normal soil were used for Fe concentration determination. As expected, overexpression plants have higher Fe content than wild-type plants, and the Fe concentration is particularly high in *Pro$_{35S}$:Myc-bHLH34#3* and *Pro$_{35S}$:Myc-bHLH104#5* plants (Fig. 5D). In contrast, the concentration

of manganese, copper, and zinc in overexpression plants is comparable to that in the wild type (Supplemental Fig. S9). These data imply that the visible phenotypes may be linked with the high transgene abundance and high Fe concentration.

Correspondingly, we examined the transcript abundance of Fe deficiency-responsive genes. In contrast to the *bhlh34bhlh104* mutants, overexpression plants constitutively activate *FIT*, *bHLH38/39/100/101*, *MYB10/72*, *IRT1*, and *FRO2* (Fig. 6) as well as *NAS2*, *NAS4*, *ZIF1*, *FRD3*, *OPT3*, and *PYE* (Supplemental Fig. S10). These data suggest that bHLH34 and bHLH104 positively regulate the Fe deficiency response.

bHLH34 and bHLH104 Directly Regulate the Transcription of *bHLH38/39/100/101*

Although *bHLH38/39/100/101* and *FIT* are the major regulators of Fe homeostasis, their transcripts are still upregulated in response to Fe deficiency. This implies that unidentified transcription factors activate their transcription in Fe-deficient conditions. Our yeast one-hybrid assays indicated that bHLH34 and bHLH104 can bind to the promoter of *bHLH101*. Considering the fact that the transcript abundance of *bHLH38/39/100/101* and *FIT* is decreased in the *bhlh34bhlh104* mutants, we proposed that *bHLH38/39/100/101* and *FIT* are the direct target genes of bHLH34 and bHLH104. To confirm this hypothesis, we designed a reporter-effector transient expression assay system (Fig. 7A; Supplemental Fig. S11A). The promoter of *bHLH101* was fused with the *GFP* reporter gene containing an NLS for construction of the reporter expression cassette, $Pro_{bHLH101}$:*NLS-GFP*. For the construction of effectors, *bHLH34* and *bHLH104* were fused with the CaMV 35S promoter to form Pro_{35S}:*Myc-bHLH34* and Pro_{35S}:*Myc-bHLH104*. When the $Pro_{bHLH101}$:*NLS-GFP* reporter was coexpressed separately with the empty vector (the backbone vector of Pro_{35S}:*Myc-bHLH34* and Pro_{35S}:*Myc-bHLH104*), only a weak GFP signal was observed (Fig. 7B). In contrast, the Pro_{35S}:*Myc-bHLH34* or Pro_{35S}:*Myc-bHLH104* effector dramatically enhanced the GFP signal of the $Pro_{bHLH101}$:*NLS-GFP* reporter. To confirm the activation specificity, we also constructed a Pro_{35S}:*Myc-MYC2* effector. MYC2 is a bHLH transcription factor with transcription activation activity (Fernández-Calvo et al., 2011). Coexpression assays indicated that use of the Pro_{35S}:*Myc-MYC2* effector resulted in as low a GFP signal as was observed for the empty vector (Fig. 7B). We further quantified the *GFP* transcript levels, which showed that the *GFP* mRNA abundance was increased

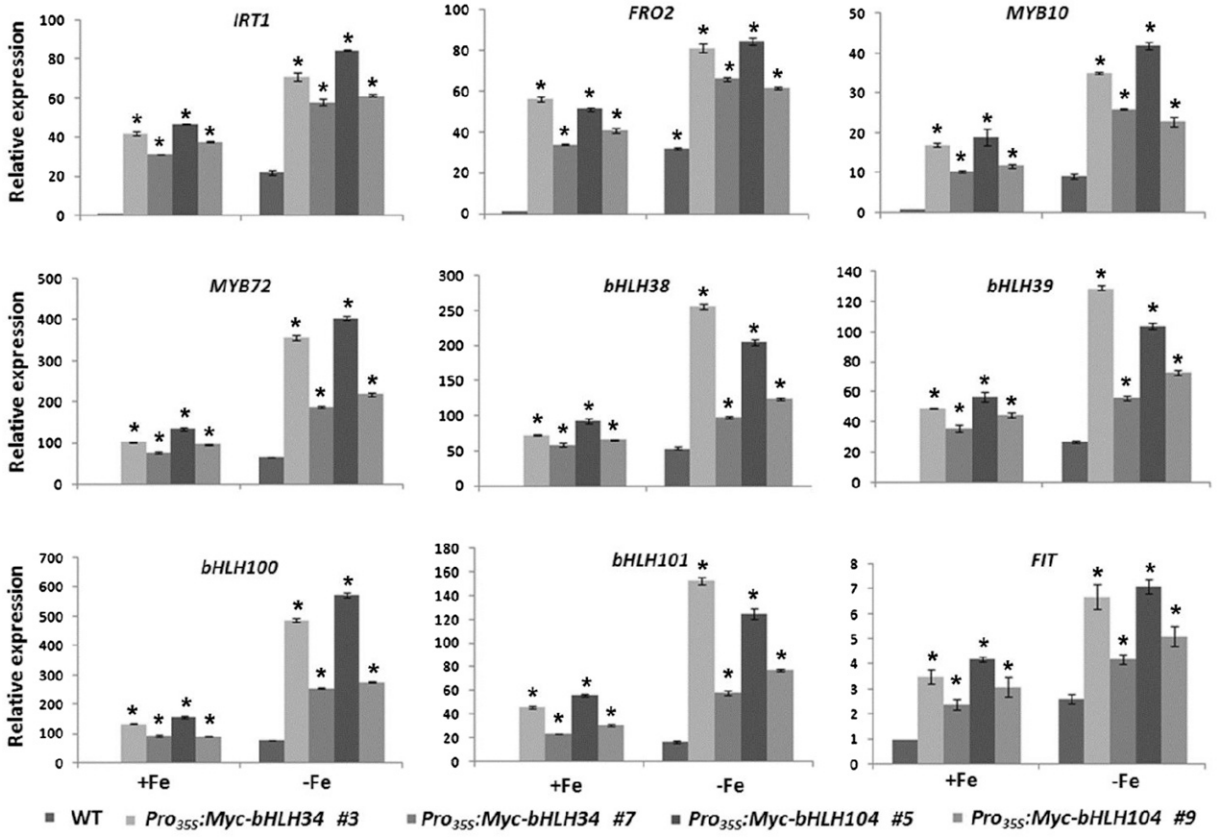

Figure 6. Expression of Fe deficiency-responsive genes in various transgenic plants. Wild-type (WT) and transgenic plants were grown on Fe-sufficient (+Fe) medium for 10 d and then transferred to +Fe or Fe-deficient (–Fe) medium for 3 d. RNA was prepared from root tissues. The data represent means ± SD of three technical repeats from one representative experiment. Significant differences from the corresponding wild type are indicated by asterisks ($P < 0.05$).

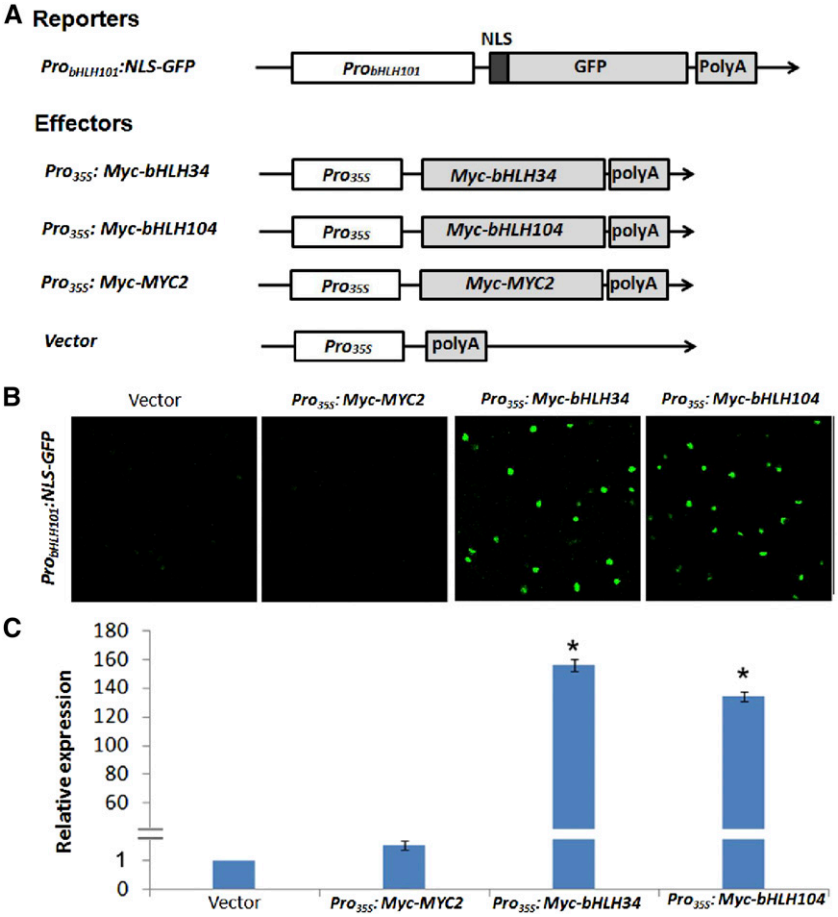

Figure 7. bHLH34 and bHLH104 activate the promoter of *bHLH101*. A, Schematic representation of the constructs used for transient expression assays. The reporter construct consists of a *bHLH101* promoter, a nuclear localization sequence (NLS) fused with the *GFP* coding sequence, and a poly(A) terminator. Effector constructs express *Myc-bHLH34*, *Myc-bHLH104*, and *Myc-MYC2* under the control of the cauliflower mosaic virus (CaMV) 35S promoter. B, bHLH34 and bHLH104 activate the promoter of *bHLH101* in transient expression assays. The results are one representative of three biological repeats. C, *GFP* transcript abundance. In the transient assays, Pro_{35S}:*Myc-GUS* was expressed as a control. *GFP* transcript abundance was normalized to *GUS* transcript. The value with the empty vector as an effector was set to 1. The results are means ± SD of three technical repeats from one of three biological repeats. Significant differences from the empty vector are indicated by asterisks ($P < 0.05$).

considerably when Pro_{35S}:*Myc-bHLH34* or Pro_{35S}:*Myc-bHLH104* was coexpressed with $Pro_{bHLH101}$:*NLS-GFP* (Fig. 7C). Correspondingly, we also constructed Pro_{bHLH38}:*NLS-GFP*, Pro_{bHLH39}:*NLS-GFP*, $Pro_{bHLH100}$:*NLS-GFP*, and Pro_{FIT}:*NLS-GFP* reporters, finding that Pro_{35S}:*Myc-bHLH34* and Pro_{35S}:*Myc-bHLH104* activated Pro_{bHLH38}:*NLS-GFP*, Pro_{bHLH39}:*NLS-GFP*, and $Pro_{bHLH100}$:*NLS-GFP* but not Pro_{FIT}:*NLS-GFP* (Supplemental Fig. S11B). These data suggest that both bHLH34 and bHLH104 specifically activate the transcription of *bHLH38/39/100/101*.

Overexpression of *bHLH101* Partially Rescues *bhlh34bhlh104* Mutants

Previous studies have confirmed that the *FRO2* and *IRT1* genes are regulated directly by bHLH38/39/100/101 and that their expression is decreased drastically in a *bHLH39*, *bHLH100*, and *bHLH101* triple knockout mutant (Yuan et al., 2008; Wang et al., 2013). Thus, we speculated that the inability of *bhlh34bhlh104* to induce *bHLH38/39/100/101* is the primary reason for the Fe deficiency symptoms and the reduced expression of *FRO2* and *IRT1* in the *bhlh34bhlh104* mutants. It was expected that elevated expression of *bHLH38/39/100/101* would cure or relieve the Fe deficiency symptoms. Because of the functional redundancy of *bHLH38/39/100/101* (Wang et al., 2013), we selected *bHLH101* as a representative. We employed the CaMV 35S promoter to drive the expression of *bHLH101*. The Pro_{35S}:*bHLH101* cascade was introduced into the *bhlh34bhlh104* mutants by *Agrobacterium tumefaciens*. Of the 78 transgenic plants screened, 42 showed significant relief of the leaf chlorosis symptom. Transcript level analysis indicated that *bHLH101* was constitutively overexpressed in the *bhlh34bhlh104*/Pro_{35S}:*bHLH101* plants (Supplemental Fig. S12A). The T2 generation plants from two different transgenic lines, *bhlh34bhlh104*/Pro_{35S}:*bHLH101#1* and *bhlh34bhlh104*/Pro_{35S}:*bHLH101#11*, were used for further analyses. When grown for 10 d on Fe-deficient medium, these two lines displayed significant growth advantages compared with the *bhlh34bhlh104* mutants (Fig. 8A), including increased root length and chlorophyll content (Fig. 8, B and C). We further assessed the expression of *IRT1*, *FRO2*, *MYB10*, and *MYB72*, finding that *IRT1* and *FRO2*, but not *FIT*, *MYB10*, and *MYB72*, were elevated in the two transgenic lines exposed to Fe-deficient conditions compared with the *bhlh34bhlh104* mutants (Fig. 8D; Supplemental Fig. S12, B–D). These data reveal that the overexpression of *bHLH101* partially rescues the *bhlh34bhlh104* mutants.

bHLH34 Can Interact Physically with bHLH104

bHLH34 and bHLH104 belong to the IVc bHLH subgroup (Heim et al., 2003). A typical feature of bHLH

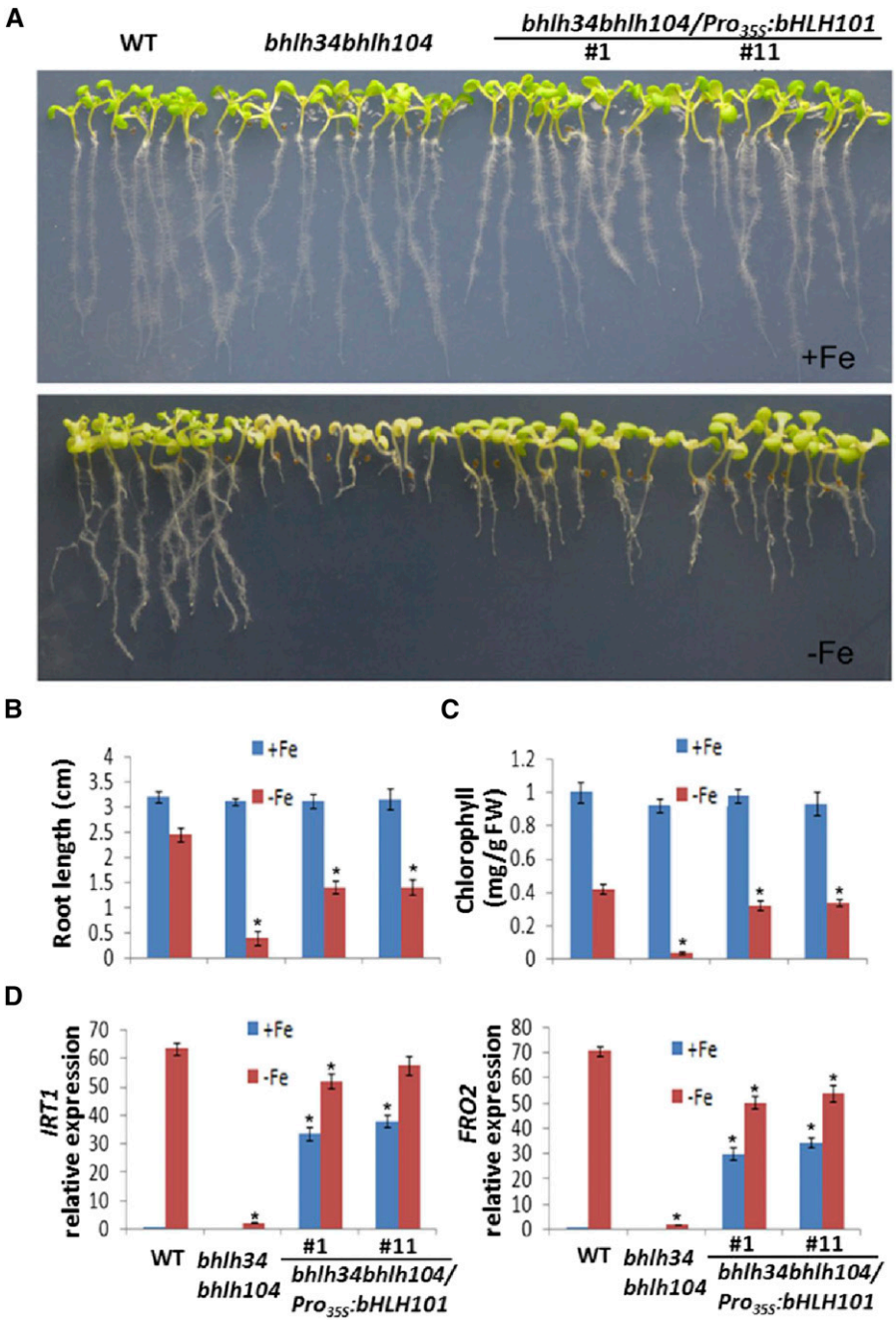

Figure 8. Overexpression of *bHLH101* partially rescues *bhlh34bhlh104*. A, Ten-day-old seedlings grown on Fe-sufficient (+Fe) or Fe-deficient (–Fe) medium. B, Root length of seedlings on +Fe or –Fe medium. Values are means ± SD of 10 plants for each genotype. C, Chlorophyll content of seedlings on +Fe or –Fe medium. Significant differences from the wild type (WT) are indicated by asterisks ($P < 0.05$). D, Expression of *IRT1* and *FRO2*. Plants were grown on +Fe medium for 10 d and then transferred to +Fe or –Fe medium for 3 d. RNA was prepared from root tissues. Significant differences from the corresponding wild type are indicated by asterisks ($P < 0.05$).

proteins is the formation of homodimers or heterodimers. To investigate the potential interaction between bHLH34 and bHLH104, we conducted yeast two-hybrid assays (Fig. 9A). When full-length bHLH34 was fused with the binding domain of GAL4 in vector pGBK-T7, it showed strong autoactivation activity. In contrast, the C-terminal truncated versions containing the bHLH domain (bHLH34C) displayed no autoactivation activity; this form was used in the subsequent yeast two-hybrid assays. A protein interaction test in yeast indicated that bHLH34C can interact with bHLH104.

Next, we employed bimolecular fluorescence complementation (BiFC) assays to confirm their interaction in plant cells. bHLH34 and bHLH104 were fused with the N-terminal fragment (nYFP) and C-terminal fragment (cYFP) of yellow fluorescent protein, respectively. When bHLH34-nYFP was transiently coexpressed with bHLH104-cYFP, strong YFP fluorescence was visible in the nucleus of epidermal cells in *Nicotiana benthamiana* leaves, whereas no YFP fluorescence was detected in negative controls (bHLH34-nYFP coexpressed with cYFP or nYFP coexpressed with bHLH104-cYFP; Fig. 9B).

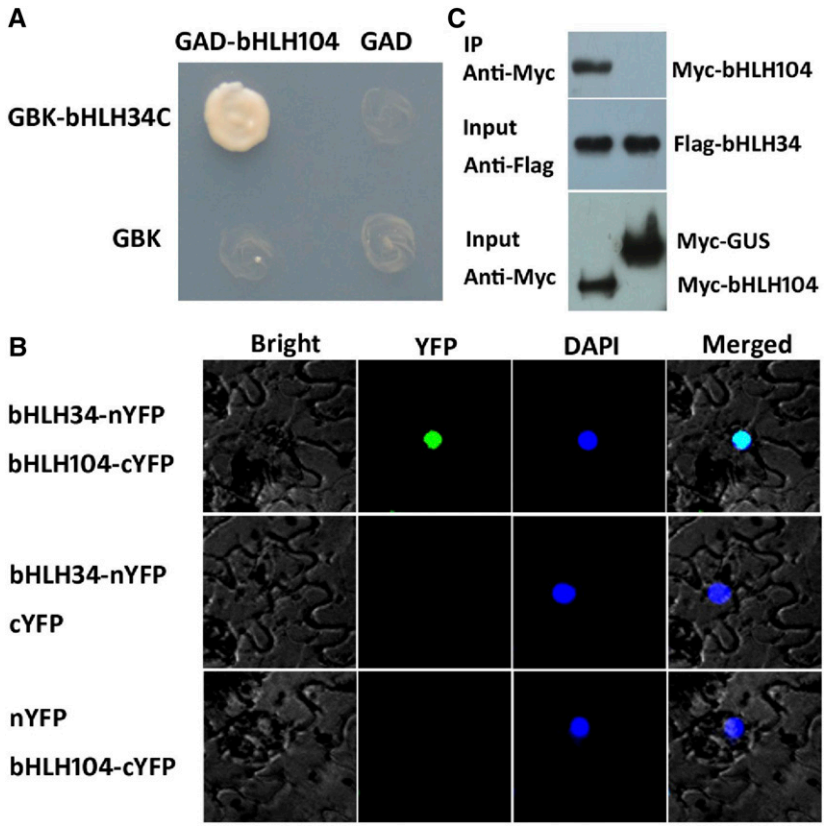

Figure 9. Interaction between bHLH34 and bHLH104. A, Yeast two-hybrid assays. Representative growth status of yeast cells is shown on synthetic dextrose medium agar plates without Leu/Trp/His/adenine. B, BiFC assays. *N. benthamiana* leaves were infiltrated with different combinations of the constructs. C, Coimmunoprecipitation (IP) assays. Total protein was immunoprecipitated using Flag antibody, and coimmunoprecipitated protein was then detected using Myc antibody.

To further confirm whether bHLH34 and bHLH104 form a protein complex in plant cells, we performed coimmunoprecipitation assays (Fig. 9C). bHLH34 and bHLH104 were transiently coexpressed in *N. benthamiana* leaves. The total proteins were incubated with Flag antibody and A/G-agarose beads and then separated by SDS-PAGE for immunoblotting with Myc antibody. In agreement with the results from BiFC, bHLH34 and bHLH104 were present in the same protein complex. Taken together, these data suggest that bHLH34 could interact physically with bHLH104.

Interaction between bHLH34/bHLH104 and bHLH105

This work confirms the interaction between bHLH34 and bHLH104. A recent study suggested that bHLH104 interacts with bHLH105 and modulates Fe homeostasis in Arabidopsis (Zhang et al., 2015). Considering that these three proteins share the same target genes (*bHLH38/39/100/101*) and their overexpressors up-regulate the same Fe deficiency-responsive genes, we proposed that they function as heterodimers. To investigate our hypothesis, yeast two-hybrid assays were performed. As shown in Figure 10A, each of these three proteins can interact with itself and the other two proteins, implying that they function as homodimers or heterodimers.

To further investigate their genetic interactions, we further produced two double mutants, *bhlh34bhlh105* and *bhlh104bhlh105*. We tried to generate *bhlh34bhlh104bhlh105* triple mutants but failed. Then, we evaluated the Fe deficiency tolerance ability of various mutants. We found that, under Fe deficiency conditions, both *bhlh34bhlh105* and *bhlh104bhlhl105* double mutants displayed the enhanced Fe deficiency symptoms (shorter roots) compared with the three single mutants (Fig. 10B). The expression of Fe deficiency-responsive genes was lower in the *bhlh34bhlh105* and *bhlh104bhlhl105* double mutants than in the three single mutants (Supplemental Fig. S13). All these data suggest that bHLH34, bHLH104, and bHLH105 play nonredundant but additive roles in modulating Fe homeostasis.

Given their similar molecular functions, we wanted to know whether the expression patterns of these three genes are different. We constructed Pro_{bHLH34}:*GUS*, $Pro_{bHLH104}$:*GUS*, and $Pro_{bHLH105}$:*GUS* transgenic plants. Although different expression strengths were observed, *bHLH34*, *bHLH104*, and *bHLH105* have similar tissue-specific expression patterns in rosette leaves, cauline leaves, stems, and siliques but not in flowers (Supplemental Fig. S14A). When seedlings were further analyzed by microscope, all plants contained GUS staining in the pericycle of the root maturation zone and veins of leaves (Fig. 11). $Pro_{bHLH105}$:*GUS* was detected in the elongation zone of root tips and early lateral roots, whereas Pro_{bHLH34}:*GUS* and $Pro_{bHLH104}$:*GUS* were not observed. In contrast, Pro_{bHLH34}:*GUS* and $Pro_{bHLH104}$:*GUS* were detected in the hypocotyls, whereas $Pro_{bHLH105}$:*GUS* was not. The difference in tissue-specific expression patterns may explain the functional nonredundancy

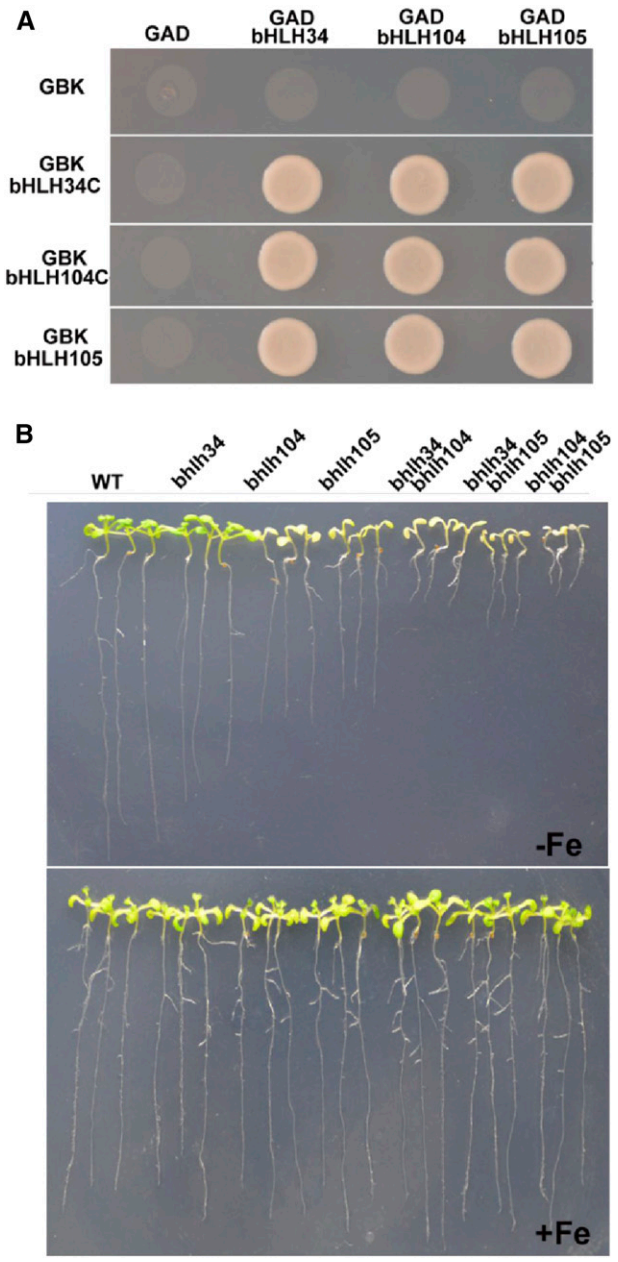

Figure 10. Interactions between bHLH34, bHLH104, and bHLH105. A, Yeast two-hybrid assays. Interaction was indicated by the ability of cells to grow on synthetic dropout medium lacking Leu/Trp/His/adenine. C-terminally truncated *bHLH34* and *bHLH104* and full-length *bHLH105* were cloned into pGBKT7, and full-length cDNAs of *bHLH34*, *bHLH104*, and *bHLH105* were cloned into pGADT7. B, Fe deficiency symptoms of various single and double mutants. Ten-day-old seedlings were germinated directly on Fe-deficient (–Fe) or Fe-sufficient (+Fe) medium. WT, Wild type.

between *bHLH34*, *bHLH104*, and *bHLH105*. In addition, GUS staining of seedlings exposed to Fe-sufficient and Fe-deficient conditions suggests that their promoter activity is stable irrespective of the Fe status (Supplemental Fig. S14B).

DISCUSSION

Fe is indispensable for plant growth and development. Fe deficiency often causes delayed growth and reduced photosynthesis and, hence, decreased crop yields. When suffering from a Fe-deficient environment, plants can sense external Fe status and employ transcription factors and intricate mechanisms to regulate the expression of Fe uptake-associated genes, which then facilitate Fe influx from soils to meet the internal demands of the plant. However, excess Fe is toxic to plant cells, owing to the generation of hydroxyl radicals by the Fenton reaction (Thomine and Vert, 2013). Therefore, it is crucial to maintain Fe homeostasis in plants. Plants have evolved sophisticated regulatory mechanisms to maintain Fe homeostasis. It is well known that bHLH38/39/100/101 and FIT have synergistic effects on the regulation of Fe deficiency responses. Their cooverexpression constitutively activates Fe acquisition strategy I in Arabidopsis. It is noteworthy that, like other Fe deficiency-responsive genes, *bHLH38/39/100/101* and *FIT* are induced by Fe deficiency. Thus, to reveal how *bHLH38/39/100/101* and *FIT* are activated in Fe-deficient conditions would provide insights into the mechanism that plants employ to maintain Fe homeostasis. Here, we characterized that both bHLH34 and bHLH104 activate the transcription of *bHLH38/39/100/101* and that they nonredundantly regulate Fe deficiency responses in Arabidopsis.

bHLH34 was identified by screening proteins that bound to the promoter of the *bHLH101* gene. The *bhlh34*, *bhlh104*, and *bhlh34bhlh104* mutants display sensitivity to Fe deficiency, including reduced root length, chlorotic leaves, and decreased ferric chelate reductase activity (Figs. 2C and 3B). Correspondingly, *amiR-bhlh34/104* plants show phenotypes similar to those of *bhlh34bhlh104* mutants (Fig. 2D; Supplemental Fig. S3D). These data indicate that loss of function of *bHLH34* and *bHLH104* causes sensitivity to Fe deficiency. Fe deficiency sensitivity can be caused by limited Fe uptake or disrupted Fe distribution. For example, *irt1*, *frd1*, and *fit* mutants display severe Fe deficiency sensitivity because of Fe uptake limitation (Robinson et al., 1999; Vert et al., 2002; Colangelo and Guerinot, 2004). In contrast, the *frd3* and *opt3* mutations enhance Fe deficiency sensitivity by disrupting Fe translocation (Durrett et al., 2007; Zhai et al., 2014). The determination of Fe concentration confirms that the *bhlh34bhlh104* mutants contain less Fe than wild-type plants in both Fe-sufficient and Fe-deficient conditions (Fig. 3, C and D), suggesting that limited Fe uptake contributes to the Fe deficiency sensitivity of the *bhlh34bhlh104* mutants. We also observed that new leaves of *bhlh34bhlh104* mutants are yellower than old leaves (Fig. 2D), whereas the opposite phenomenon occurs in the *bHLH34* and *bHLH104* overexpression plants (Fig. 5A), implying that bHLH34 and bHLH104 may interrupt Fe distribution between leaves.

Fe deficiency-responsive genes, including *IRT1*, *FRO2*, *MYB10/72*, *FIT*, and *bHLH38/39/100/101*, are

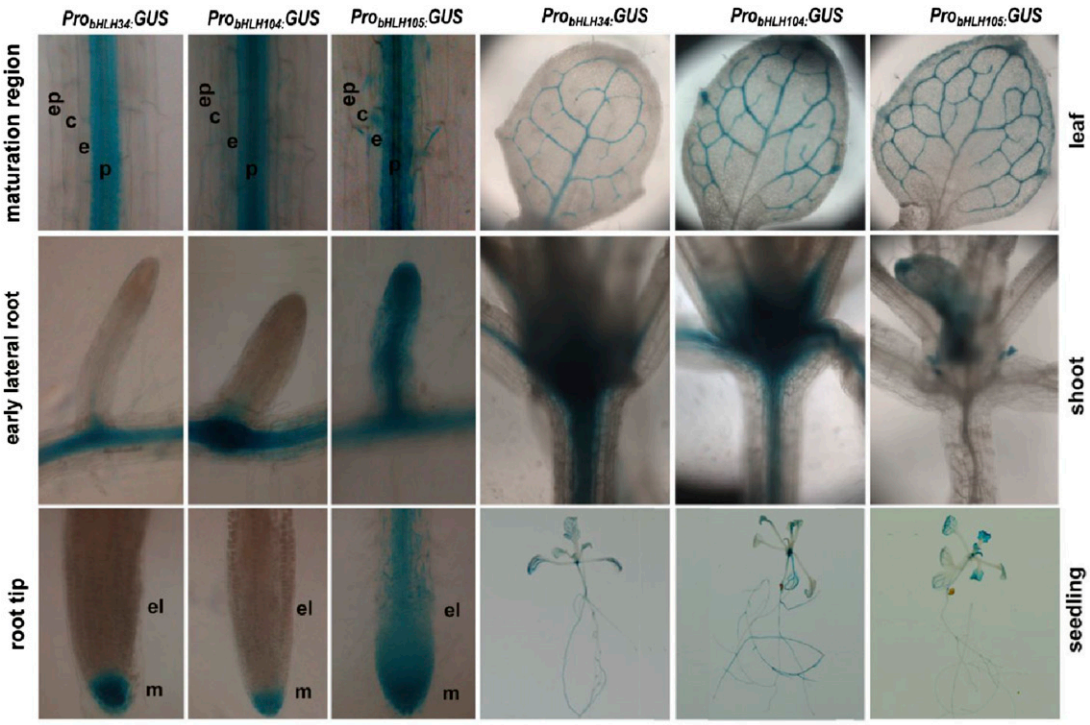

Figure 11. GUS staining of Pro_{bHLH34}:*GUS*, $Pro_{bHLH104}$:*GUS*, and $Pro_{bHLH105}$:*GUS* seedlings. Two-week-old seedlings were used for GUS staining. GUS staining of the root maturation regions, early lateral roots, root tips, leaves, hypocotyls, and whole seedlings is shown. c, Cortex; e, endodermis; el, elongation region of the root tip; ep, epidermis; m, meristem zone of the root tip; p, pericycle.

repressed in the *bhlh34bhlh104* mutants (Fig. 4), indicating that the loss of function of *bHLH34* and *bHLH104* impairs the transduction of Fe deficiency response signaling. Although *bhlh34* and *bhlh104* mutants display reduced activation of Fe deficiency-responsive genes, the *bhlh34bhlh104* mutants have the strongest inhibitory effect on the Fe deficiency-responsive genes. When either Pro_{bHLH34}:*Myc-bHLH34* or $Pro_{bHLH104}$:*Myc-bHLH104* was introduced into *bhlh34bhlh104* double mutants, the Fe deficiency symptoms of *bhlh34bhlh104* were partially rescued (Supplemental Fig. S15). These data suggest that *bHLH34* and *bHLH104* have nonredundant functions under Fe-deficient conditions. In contrast to *bhlh34* and *bhlh104* mutants, *bHLH34* and *bHLH104* overexpression plants activate the expression of Fe deficiency-responsive genes (Fig. 6). In agreement with this, Fe is overaccumulated in the overexpression plants (Fig. 5D). Taken together, our data suggest that bHLH34 and bHLH104 act as positive regulators in Fe deficiency response signaling.

The *bhlh34bhlh104* mutants displayed enhanced Fe deficiency sensitivity. However, unexpectedly, we found that about 10% of Pro_{35S}:*Myc-bHLH34* and 30% of Pro_{35S}:*Myc-bHLH104* plants showed short roots on Fe-deficient medium, although they accumulated high Fe content and activated Fe deficiency-responsive genes, including *bHLH38/39/100/101*, *MYB10/72*, *FRO2*, and *IRT1*. In fact, similar observations were made for the *pye1* mutant, which up-regulates Fe deficiency-responsive genes and accumulates excessive Fe but displays short roots under Fe deficiency conditions (Long et al., 2010). *NAS4* and *ZIF1* are significantly up-regulated in the *bHLH34* and *bHLH104* overexpression plants and particular high when overexpression plants are subjected to Fe deficiency conditions (Supplemental Fig. S10). It is noteworthy that *NAS4* and *ZIF1* are directly negatively regulated by *PYE* (Long et al., 2010). As a negative regulator in Fe homeostasis, *PYE* is also a direct target of bHLH104 and bHLH105 (Zhang et al., 2015). Our results suggest that *PYE* is positively regulated by bHLH34, bHLH104, and bHLH105. The expression analysis of *NAS4* and *ZIF1* between *bhlh34bhlhl104* and *pye1* mutants (Supplemental Fig. S16) indicates that *NAS4* and *ZIF1* are positively and negatively regulated by bHLH34/bHLH104 and PYE, respectively. Plants have evolved this mechanism to fine-tune Fe homeostasis.

Recently, Zhang et al. (2015) revealed that overexpression of *bHLH104* and *bHLH105* activates the Fe deficiency-responsive genes and overaccumulation of Fe. However, the Fe deficiency sensitivity of our overexpression plants is completely different from the results of Zhang et al. (2015), who confirmed that *bHLH104* overexpression plants produced longer roots than the wild type on Fe-deficient medium. They used Pro_{35S}:*bHLH104-GFP* as an overexpression construct, whereas we used Pro_{35S}:*Myc-bHLH104*. To investigate

whether the C-terminal fused GFP affects the function of bHLH34 or bHLH104, we constructed Pro_{35S}:*Myc-bHLH34-GFP* and Pro_{35S}:*Myc-bHLH104-GFP* transgenic plants. No visible phenotype was found in all Pro_{35S}:*Myc-bHLH34-GFP* and Pro_{35S}:*Myc-bHLH104-GFP* transgenic plants compared with the wild type when plants were grown in normal soils. In agreement with the results from Zhang et al. (2015), about 70% of these GFP fusion transgenic plants produced significantly longer roots than the wild type on Fe-deficient medium (Supplemental Fig. S17A). The expression of Fe deficiency-responsive genes in GFP fusion transgenic plants with longer roots is significantly lower than that in Myc fusion transgenic plants with shorter roots, but it is comparable to the Myc fusion transgenic plants with normal roots (Supplemental Fig. S17B). It is noteworthy that the overexpression plants with visible phenotypes have extremely high transgene levels compared with overexpressors with invisible phenotypes (Fig. 5C; Supplemental Fig. S8B). Therefore, it is likely that the extremely high expression of transgene caused abnormal regulation of Fe uptake-associated genes and Fe overload. In any case, it is an efficient approach to generate Fe deficiency-tolerant plants by constitutively expressing *bHLH34* or *bHLH104* with a C terminus fused with a *GFP* gene.

Under both Fe-sufficient and Fe-deficient conditions, the transcript levels of *bHLH38/39/100/101* are always lower in the *bhlh34*, *bhlh104*, and *bhlh34bhlh104* mutants than in wild-type plants (Fig. 4). Transient expression assays reveal that both bHLH34 and bHLH104 activate the promoters of *bHLH38/39/100/101* (Fig. 7, B and C; Supplemental Fig. S11). These data suggest that bHLH34 and bHLH104 directly and positively regulate the transcription of *bHLH38/39/100/101*. In agreement with our results, Zhang et al. (2015) showed the direct regulation of *bHLH38/39/100/101* by bHLH104. *bHLH38/39/100/101* are strongly induced when wild-type plants are exposed to Fe-deficient conditions. However, it is worth noting that, in some mutants where Fe homeostasis is disrupted, such as *irt1*, *frd1*, *frd3*, and *fit*, *bHLH38/39/100/101* transcript abundance is increased even under Fe-sufficient conditions compared with wild-type plants (Wang et al., 2007). The fact that Fe deficiency-responsive genes are regulated by internal Fe demand via shoot-to-root signaling was demonstrated previously (Grusak and Pezeshgi, 1996; Vert et al., 2003). Interestingly, although the *bhlh34bhlh104* mutants have lower Fe content than wild-type plants, the induction of *bHLH38/39/100/101* by Fe deficiency is strongly inhibited in the *bhlh34bhlh104* mutants, suggesting that the transcriptional activation of *bHLH38/39/100/101* by internal Fe demand is largely dependent on *bHLH34* and *bHLH104*.

It has been confirmed that *bHLH38/39/100/101* have redundant functions in the Fe deficiency response (Yuan et al., 2008; Wang et al., 2013). Our experiments indicate that the constitutive expression of *bHLH101* partially rescued the severe Fe deficiency symptoms of *bhlh34bhlh104* mutants (Fig. 8), implying that the regulation of *bHLH38/39/100/101* by bHLH34 and bHLH104 is required for Fe homeostasis. Because of the imperfect complementation by overexpression of *bHLH101*, it is possible that the ectopic expression of *bHLH101* caused ectopic expression of its target genes, which then led to the abnormal Fe distribution, or that bHLH34 and bHLH104 also regulate other genes that are involved in Fe homeostasis but are not regulated by bHLH101. In fact, we found that the induction of *FIT*, *MYB10*, and *MYB72* by Fe deficiency is not rescued in *bhlh34bhlh104/*Pro_{35S}:*bHLH101#1* and *bhlh34bhlh104/*Pro_{35S}:*bHLH101#11* plants (Supplemental Fig. S12). It has been reported that *MYB10* and *MYB72* are required for growth in Fe-limiting conditions by directly regulating the expression of *NAS4* (Palmer et al., 2013). *NAS* genes are responsible for the synthesis of nicotianamine, which plays a role in the intercellular and intracellular distribution of Fe (Takahashi et al., 2003; Klatte et al., 2009). Therefore, the elevated expression of *bHLH101* may rescue only the Fe uptake phenotype, but not the Fe distribution phenotype, in the *bhlh34bhlh104* mutants. The transcript abundance of *bHLH34* and *bHLH104* is not induced by Fe deficiency (Supplemental Fig. S2), which implies that they may be regulated at the posttranscriptional level because their

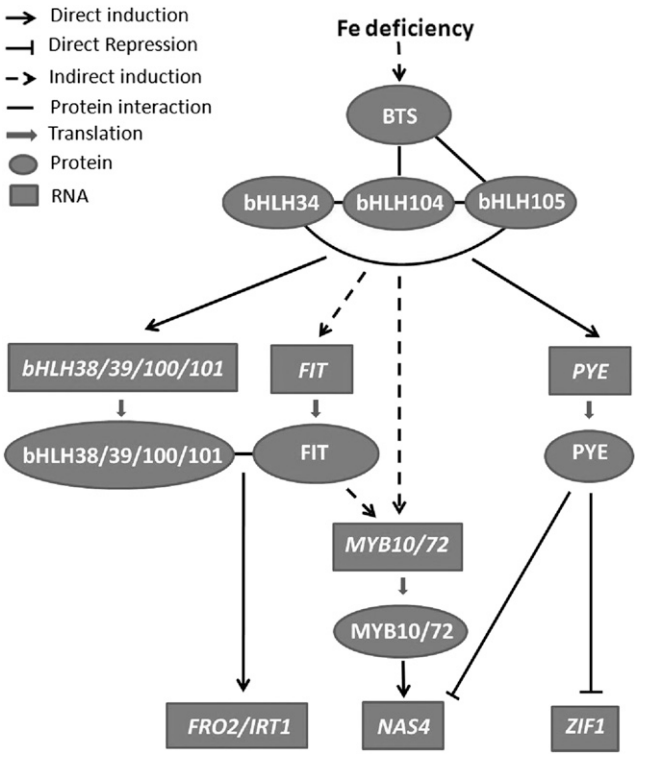

Figure 12. Fe deficiency-responsive signaling pathway. Fe deficiency stabilizes the BTS protein that interacts with bHLH104 and bHLH105. bHLH34, bHLH104, and bHLH105 can form homodimers or heterodimers to activate the transcription of *bHLH38/39/100/101* and *PYE*. FIT interacts with bHLH38/39/100/101 to activate the transcription of *FRO2* and *IRT1*. PYE regulates the expression of *ZIF1* and *NAS4* negatively. MYB10 and MYB72 regulate the expression of *NAS4* positively. The induction of *MYB10/72* by Fe deficiency is partially dependent on FIT; bHLH34/104/105 are required for the induction of *FIT* and *MYB10/72*.

target genes are up-regulated by Fe deficiency. To further analyze their protein stability and screen their interaction partners will provide insights into their regulation mechanisms under Fe deficiency conditions. The stronger Fe deficiency symptoms of double mutants than single mutants suggest that bHLH34, bHLH104, and bHLH105 play nonredundant roles in regulating Fe homeostasis. We also observed differential expression patterns among Pro_{bHLH34}:*GUS*, $Pro_{bHLH104}$:*GUS*, and $Pro_{bHLH105}$:*GUS*, which might explain the nonredundant roles.

A putative Fe deficiency-responsive signaling pathway is shown in Figure 12. BTS is considered a potential Fe sensor because its structure, its ability to bind Fe, and its capacity to catalyze ubiquitination are similar to the mammalian Fe sensor FBXL5 (Kobayashi et al., 2013; Selote et al., 2015). *BTS* is induced and its product is stabilized by Fe deficiency; however, it has been confirmed to negatively regulate Fe homeostasis (Long et al., 2010; Selote et al., 2015; Zhang et al., 2015). Long et al. (2010) confirmed that bHLH104 and bHLH105, but not bHLH34, interact with BTS in yeast. Although its interacts with BTS, bHLH104 protein is not affected by BTS (Selote et al., 2015). bHLH34, bHLH104, and bHLH105 function as homodimers or heterodimers. It is likely that the interaction of BTS with bHLH104 competitively interferes with the formation of dimers, which then affects the regulation of downstream genes, such as *bHLH38/39/100/101* and *PYE*. FIT interacts with bHLH38/39/100/101 to activate the expression of *IRT1* and *FRO2*. PYE functions as the negative regulator of *ZIF1* and *NAS4*. MYB10 and MYB72 function redundantly to regulate Fe homeostasis by the direct activation of *NAS4*. The induction of *MYB10/72* by Fe deficiency is partially dependent on FIT, and bHLH34/104/105 are required for the induction of *FIT* and *MYB10/72*. It is worth mentioning that the model has no spatial dimension; it reflects interactions globally but is not applicable in any particular cell type, because the expression patterns of the different players do not always overlap. Future research should aim at identifying the distinct modules that are active in the root cortex and epidermis, in the root stele, and in various leaf cell types.

MATERIALS AND METHODS

Plant Materials and Growth Conditions

The Arabidopsis (*Arabidopsis thaliana*) ecotype Columbia-0 was used as the wild type in this study. The T-DNA insertion lines for *bHLH34* (CS411089), *bHLH104* (Salk_099496C), and *bHLH105* (Salk_043690C) were confirmed using PCR with a T-DNA primer and gene-specific primers (Supplemental Table S1). *pye1* was described previously (Long et al., 2010). Plants were grown in long photoperiods (16 h of light/8 h of dark) or in short photoperiods (8 h of light/16 h of dark) at 22°C. Surface-sterilized seeds were stratified at 4°C for 2 to 4 d before being planted on medium. Fe-sufficient medium is one-half-strength Murashige and Skoog (MS) medium with 1% (w/v) Suc, 0.8% (w/v) agar, and 0.1 mM FeEDTA. Fe-deficient medium is the same without FeEDTA.

Plasmid Construction

Standard molecular biology techniques were used for the cloning procedures. Genomic DNA from Arabidopsis was used as the template for amplification of the upstream regulatory promoter sequence for Pro_{bHLH34}:*GUS*, $Pro_{bHLH104}$:*GUS*, $Pro_{bHLH105}$:*GUS*, Pro_{FIT}:*NLS-GFP*, Pro_{bHLH38}:*NLS-GFP*, Pro_{bHLH39}:*NLS-GFP*, $Pro_{bHLH100}$:*NLS-GFP*, and $Pro_{bHLH101}$:*NLS-GFP*. The NLS was amplified from the pGADT7 plasmid. For Pro_{35S}:*Flag-bHLH34*, Pro_{35S}:*Myc-bHLH34*, Pro_{35S}:*Myc-bHLH104*, Pro_{35S}:*bHLH101*, Pro_{35S}:*Myc-GUS*, and Pro_{35S}:*Myc-MYC2*, the corresponding coding sequences were inserted between the CaMV 35S promoter and poly(A) of the binary vector pOCA30. *amiR-bhlh34/104* was integrated into the *MIR319a* backbone, and the construction strategy was described previously (Liang et al., 2012). Primers used for these constructs are listed in Supplemental Table S1. Arabidopsis transformation was conducted by the floral dip method (Clough and Bent, 1998). Transgenic plants were selected with the use of 50 μg mL^{-1} kanamycin.

Histochemical GUS Staining

Whole seedlings were immersed immediately in 1.5 mL of staining solution containing 0.5 mg mL^{-1} 5-bromo-4-chloro-3-indolyl-β-D-glucuronide (Sigma) in 0.1 M sodium phosphate buffer (pH 7.3) in a microfuge tube. The reaction was performed in the dark at 37°C until a blue indigo color appeared. After the reaction, seedlings were rinsed in 0.1 M sodium phosphate buffer (pH 7.3). The samples were then rinsed twice in 70% (v/v) ethanol to remove chlorophylls.

Fe Concentration Measurement

To determine Fe content, 11-d-old seedlings grown on Fe-sufficient medium were transferred to Fe-sufficient or Fe-deficient medium for 3 d. The shoots and roots were harvested separately and used for Fe measurement. Leaves of 4-week-old plants grown in normal soils were used for the measurement of Fe content. About 100 mg dry weight for roots or shoots was used as one sample, and three samples were used in each independent experiment. Fe content analysis was performed using inductively coupled plasma spectroscopy.

Ferric Chelate Reductase Assays

Ferric chelate reductase assays were performed as described previously (Yi and Guerinot, 1996). Briefly, 10 intact plants for each genotype were pretreated for 30 min in plastic vessels with 4 mL of one-half-strength MS solution without micronutrients (pH 5.5) and then soaked into 4 mL of Fe(III) reduction assay solution [one-half-strength MS solution without micronutrients, 0.1 mM Fe(III)-EDTA, and 0.3 mM ferrozine, pH adjusted to 5 with KOH] for 30 min in darkness. An identical assay solution containing no plants was used as a blank. The purple-colored Fe(II)-ferrozine complex was quantified at 562 nm.

Chlorophyll Measurement

Chlorophyll content was measured in 2-week-old plants grown on Fe-sufficient and Fe-deficient media. All leaves were collected and ground to powder in liquid nitrogen. The powder was resuspended in 80% (v/v) acetone on ice and centrifuged at 10,000*g* at 4°C for 5 min. Chlorophyll concentrations were calculated from spectroscopy absorbance measurements at 663.2, 646.8, and 470 nm (Lichtenthaler, 1987).

Gene Expression Analysis

One microgram of total RNA extracted using the Trizol reagent (Invitrogen) was used for oligo(dT)$_{18}$-primed cDNA synthesis according to the reverse transcription protocol (Fermentas). The resulting cDNA was subjected to relative quantitative PCR using the SYBR Premix Ex Taq kit (TaKaRa) on a Roche LightCycler 480 real-time PCR machine, according to the manufacturer's instructions. *ACTIN2* (*ACT2*) was amplified as an internal control, and gene copy number was normalized to that of *ACT2*. For the quantification of each gene, at least three biological repeats were used. Each biological repeat contained three technical replicates. One representative result from one biological repeat is shown. The analysis of statistical significance was performed by Student's *t* test. The quantitative reverse transcription-PCR primers are listed in Supplemental Table S1.

Yeast Assays

For the yeast one-hybrid assay, the Matchmaker Gold Yeast One-Hybrid Library Screening System (Clontech) was used. The pAbAi vector harboring a

1,000-bp sequence upstream of the *bHLH101* gene was integrated into the genome of yeast strain Y1HGold followed by selection on synthetic dextrose medium agar plates without uracil. We screened an Arabidopsis equalized full-length cDNA library on synthetic dextrose medium without Leu supplemented with 100 ng mL^{-1} aureobasidin A. The aureobasidin A resistance is activated by prey proteins that specifically interact with the bait sequence. Candidate cDNA-harboring vectors were amplified and isolated via *Escherichia coli*. The sequence of each candidate was analyzed with the help of the TAIR database.

For the yeast two-hybrid assay, C-terminally truncated *bHLH34C* and *bHLH104C* containing the bHLH domain and full-length *bHLH105* cDNAs were cloned into pGBKT7, and the full-length cDNAs of *bHLH34*, *bHLH104*, and *bHLH105* were cloned into pGADT7. Growth was determined as described in the Yeast Two-Hybrid System User Manual (Clontech). Primers used for vector construction are listed in Supplemental Table S1. Experiments were repeated three times.

Transient Expression Assays

Plasmids were transformed into *Agrobacterium tumefaciens* strain EHA105. Agrobacterial cells were infiltrated into leaves of *Nicotiana benthamiana* by the infiltration buffer (0.2 mM acetosyringone, 10 mM $MgCl_2$, and 10 mM MES, pH 5.6). For the BiFC assay, equal volumes of an *A. tumefaciens* culture were mixed before infiltration into *N. benthamiana* leaves. After infiltration, YFP and 4′,6-diaminophenylindole fluorescence were observed with a confocal laser scanning microscope (Olympus). For transcription activation assay, the final optical density at 600 nm value was 0.1 (an internal control; Pro_{35S}:*Myc-GUS*), 0.5 (reporter), or 0.5 (effector). After infiltration, plants were placed in the dark at 24°C for 48 h before RNA extraction. The transcript abundance of *GFP* was normalized to *GUS*.

Coimmunoprecipitation Assay

Flag-bHLH34 and Myc-bHLH104 (or Myc-GUS) were transiently coexpressed in *N. benthamiana* leaves. Infected leaves were harvested 48 h after infiltration and used for protein extraction. Flag-fused bHLH34 was immunoprecipitated using Flag antibody, and the coimmunoprecipitated proteins were then detected using Myc antibody.

Sequence data from this article can be found in the Arabidopsis Genome Initiative or GenBank/EMBL databases under the following accession numbers: bHLH34 (At3g23210), bHLH104 (At4g14410), bHLH105 (At5g54680), bHLH38 (At3g56970), bHLH39 (At3g56980), bHLH100 (At2g41240), bHLH101 (At5g04150), FIT (At2g28160), MYB10 (At3g12820), MYB72 (At1g56160), FRO2 (At1g01580), IRT1 (At4g19690), NAS2 (At5g56080), NAS4 (At1g56430), ZIF1 (At5g13740), FRD3 (At3g08040), OPT3 (At5g59040), PYE (At3g47640), and ACT2 (At3g18780).

Supplemental Data

The following supplemental materials are available.

Supplemental Figure S1. Phylogenetic tree of bHLH proteins involved in Fe homeostasis.

Supplemental Figure S2. Expression of *bHLH34* and *bHLH104* in response to Fe deficiency.

Supplemental Figure S3. Growth status of wild-type and mutant plants.

Supplemental Figure S4. Analysis of *amiR-bhlh34/104* and double mutant plants.

Supplemental Figure S5. Chlorophyll content of mutant seedlings on Fe-sufficient or Fe-deficient medium.

Supplemental Figure S6. *NAS2*, *NAS4*, *ZIF1*, *FRD3*, *OPT3*, and *PYE* transcript levels in various mutant plants.

Supplemental Figure S7. Complementation of *bhlh34* and *bhlh104* mutants.

Supplemental Figure S8. Analysis of *bHLH34* and *bHLH104* overexpression plants.

Supplemental Figure S9. Concentration of other metals in overexpression plants.

Supplemental Figure S10. *NAS2*, *NAS4*, *ZIF1*, *FRD3*, *OPT3*, and *PYE* transcript levels in overexpression plants.

Supplemental Figure S11. bHLH34 and bHLH104 activate the promoter of *bHLH38/39/100*.

Supplemental Figure S12. Analysis of *bhlh34bhlh104/*Pro_{35S}:*bHLH101* plants.

Supplemental Figure S13. Expression of Fe deficiency-responsive genes in various single and double mutants.

Supplemental Figure S14. GUS staining of Pro_{bHLH34}:*GUS*, $Pro_{bHLH104}$:*GUS*, and $Pro_{bHLH105}$:*GUS* plants.

Supplemental Figure S15. Partial complementation of *bhlh34blhlh104* double mutants by $Prob_{HLH34}$:*Myc-bHLH34* and $Pro_{bHLH104}$:*Myc-bHLH104*.

Supplemental Figure S16. Expression of *NAS4* and *ZIF1* in *bhlh34blhlh104* and *pye1* mutants.

Supplemental Figure S17. Phenotypes of Pro_{35S}:*Myc-bHLH34-GFP* and Pro_{35S}:*Myc-bHLH104-GFP* plants.

Supplemental Table S1. Primers used in this article.

ACKNOWLEDGMENTS

We thank TAIR at Ohio State University for the T-DNA insertion mutants.

Received November 23, 2015; accepted February 24, 2016; published February 26, 2016.

LITERATURE CITED

Clough SJ, Bent AF (1998) Floral dip: a simplified method for Agrobacterium-mediated transformation of *Arabidopsis thaliana*. Plant J **16:** 735–743

Colangelo EP, Guerinot ML (2004) The essential basic helix-loop-helix protein FIT1 is required for the iron deficiency response. Plant Cell **16:** 3400–3412

Durrett TP, Gassmann W, Rogers EE (2007) The FRD3-mediated efflux of citrate into the root vasculature is necessary for efficient iron translocation. Plant Physiol **144:** 197–205

Eide D, Broderius M, Fett J, Guerinot ML (1996) A novel iron-regulated metal transporter from plants identified by functional expression in yeast. Proc Natl Acad Sci USA **93:** 5624–5628

Fernández-Calvo P, Chini A, Fernández-Barbero G, Chico JM, Gimenez-Ibanez S, Geerinck J, Eeckhout D, Schweizer F, Godoy M, Franco-Zorrilla JM, et al (2011) The *Arabidopsis* bHLH transcription factors MYC3 and MYC4 are targets of JAZ repressors and act additively with MYC2 in the activation of jasmonate responses. Plant Cell **23:** 701–715

Gamsjaeger R, Liew CK, Loughlin FE, Crossley M, Mackay JP (2007) Sticky fingers: zinc-fingers as protein-recognition motifs. Trends Biochem Sci **32:** 63–70

Grusak MA, Pezeshgi S (1996) Shoot-to-root signal transmission regulates root Fe(III) reductase activity in the *dgl* mutant of pea. Plant Physiol **110:** 329–334

Gu Z, Steinmetz LM, Gu X, Scharfe C, Davis RW, Li WH (2003) Role of duplicate genes in genetic robustness against null mutations. Nature **421:** 63–66

Hänsch R, Mendel RR (2009) Physiological functions of mineral micronutrients (Cu, Zn, Mn, Fe, Ni, Mo, B, Cl). Curr Opin Plant Biol **12:** 259–266

Heim MA, Jakoby M, Werber M, Martin C, Weisshaar B, Bailey PC (2003) The basic helix-loop-helix transcription factor family in plants: a genome-wide study of protein structure and functional diversity. Mol Biol Evol **20:** 735–747

Henriques R, Jásik J, Klein M, Martinoia E, Feller U, Schell J, Pais MS, Koncz C (2002) Knock-out of Arabidopsis metal transporter gene IRT1 results in iron deficiency accompanied by cell differentiation defects. Plant Mol Biol **50:** 587–597

Jakoby M, Wang HY, Reidt W, Weisshaar B, Bauer P (2004) FRU (BHLH029) is required for induction of iron mobilization genes in *Arabidopsis thaliana*. FEBS Lett **577:** 528–534

Klatte M, Schuler M, Wirtz M, Fink-Straube C, Hell R, Bauer P (2009) The analysis of Arabidopsis nicotianamine synthase mutants reveals

functions for nicotianamine in seed iron loading and iron deficiency responses. Plant Physiol **150:** 257–271

Kobayashi T, Nagasaka S, Senoura T, Itai RN, Nakanishi H, Nishizawa NK (2013) Iron-binding haemerythrin RING ubiquitin ligases regulate plant iron responses and accumulation. Nat Commun **4:** 2792

Kobayashi T, Nishizawa NK (2012) Iron uptake, translocation, and regulation in higher plants. Annu Rev Plant Biol **63:** 131–152

Liang G, He H, Li Y, Yu D (2012) A new strategy for construction of artificial miRNA vectors in Arabidopsis. Planta **235:** 1421–1429

Lichtenthaler HK (1987) Chlorophylls and carotenoids: pigments of photosynthetic biomembranes. Methods Enzymol **148:** 350–382

Ling H-Q, Bauer P, Bereczky Z, Keller B, Ganal M (2002) The tomato fer gene encoding a bHLH protein controls iron-uptake responses in roots. Proc Natl Acad Sci USA **99:** 13938–13943

Long TA, Tsukagoshi H, Busch W, Lahner B, Salt DE, Benfey PN (2010) The bHLH transcription factor POPEYE regulates response to iron deficiency in *Arabidopsis* roots. Plant Cell **22:** 2219–2236

Meiser J, Lingam S, Bauer P (2011) Posttranslational regulation of the iron deficiency basic helix-loop-helix transcription factor FIT is affected by iron and nitric oxide. Plant Physiol **157:** 2154–2166

Mori S (1999) Iron acquisition by plants. Curr Opin Plant Biol **2:** 250–253

Morrissey J, Guerinot ML (2009) Iron uptake and transport in plants: the good, the bad, and the ionome. Chem Rev **109:** 4553–4567

Palmer CM, Hindt MN, Schmidt H, Clemens S, Guerinot ML (2013) MYB10 and MYB72 are required for growth under iron-limiting conditions. PLoS Genet **9:** e1003953

Robinson NJ, Procter CM, Connolly EL, Guerinot ML (1999) A ferric-chelate reductase for iron uptake from soils. Nature **397:** 694–697

Salahudeen AA, Thompson JW, Ruiz JC, Ma HW, Kinch LN, Li Q, Grishin NV, Bruick RK (2009) An E3 ligase possessing an iron-responsive hemerythrin domain is a regulator of iron homeostasis. Science **326:** 722–726

Santi S, Schmidt W (2009) Dissecting iron deficiency-induced proton extrusion in Arabidopsis roots. New Phytol **183:** 1072–1084

Selote D, Samira R, Matthiadis A, Gillikin JW, Long TA (2015) Iron-binding E3 ligase mediates iron response in plants by targeting basic helix-loop-helix transcription factors. Plant Physiol **167:** 273–286

Sivitz A, Grinvalds C, Barberon M, Curie C, Vert G (2011) Proteasome-mediated turnover of the transcriptional activator FIT is required for plant iron-deficiency responses. Plant J **66:** 1044–1052

Takahashi M, Terada Y, Nakai I, Nakanishi H, Yoshimura E, Mori S, Nishizawa NK (2003) Role of nicotianamine in the intracellular delivery of metals and plant reproductive development. Plant Cell **15:** 1263–1280

Terry N (1980) Limiting factors in photosynthesis. I. Use of iron stress to control photochemical capacity in vivo. Plant Physiol **65:** 114–120

Thomine S, Vert G (2013) Iron transport in plants: better be safe than sorry. Curr Opin Plant Biol **16:** 322–327

Varotto C, Maiwald D, Pesaresi P, Jahns P, Salamini F, Leister D (2002) The metal ion transporter IRT1 is necessary for iron homeostasis and efficient photosynthesis in *Arabidopsis thaliana*. Plant J **31:** 589–599

Vashisht AA, Zumbrennen KB, Huang X, Powers DN, Durazo A, Sun D, Bhaskaran N, Persson A, Uhlen M, Sangfelt O, et al (2009) Control of iron homeostasis by an iron-regulated ubiquitin ligase. Science **326:** 718–721

Vert G, Grotz N, Dédaldéchamp F, Gaymard F, Guerinot ML, Briat JF, Curie C (2002) IRT1, an *Arabidopsis* transporter essential for iron uptake from the soil and for plant growth. Plant Cell **14:** 1223–1233

Vert GA, Briat JF, Curie C (2003) Dual regulation of the Arabidopsis high-affinity root iron uptake system by local and long-distance signals. Plant Physiol **132:** 796–804

Walker EL, Connolly EL (2008) Time to pump iron: iron-deficiency-signaling mechanisms of higher plants. Curr Opin Plant Biol **11:** 530–535

Wang HY, Klatte M, Jakoby M, Bäumlein H, Weisshaar B, Bauer P (2007) Iron deficiency-mediated stress regulation of four subgroup Ib BHLH genes in *Arabidopsis thaliana*. Planta **226:** 897–908

Wang N, Cui Y, Liu Y, Fan H, Du J, Huang Z, Yuan Y, Wu H, Ling HQ (2013) Requirement and functional redundancy of Ib subgroup bHLH proteins for iron deficiency responses and uptake in Arabidopsis thaliana. Mol Plant **6:** 503–513

Yi Y, Guerinot ML (1996) Genetic evidence that induction of root Fe(III) chelate reductase activity is necessary for iron uptake under iron deficiency. Plant J **10:** 835–844

Yuan Y, Wu H, Wang N, Li J, Zhao W, Du J, Wang D, Ling HQ (2008) FIT interacts with AtbHLH38 and AtbHLH39 in regulating iron uptake gene expression for iron homeostasis in Arabidopsis. Cell Res **18:** 385–397

Yuan YX, Zhang J, Wang DW, Ling HQ (2005) AtbHLH29 of Arabidopsis thaliana is a functional ortholog of tomato FER involved in controlling iron acquisition in strategy I plants. Cell Res **15:** 613–621

Zhai Z, Gayomba SR, Jung HI, Vimalakumari NK, Piñeros M, Craft E, Rutzke MA, Danku J, Lahner B, Punshon T, et al (2014) OPT3 is a phloem-specific iron transporter that is essential for systemic iron signaling and redistribution of iron and cadmium in *Arabidopsis*. Plant Cell **26:** 2249–2264

Zhang J, Liu B, Li M, Feng D, Jin H, Wang P, Liu J, Xiong F, Wang J, Wang HB (2015) The bHLH transcription factor bHLH104 interacts with IAA-LEUCINE RESISTANT3 and modulates iron homeostasis in *Arabidopsis*. Plant Cell **27:** 787–805